Interfacial Tension of Two Ionic Liquids, 1-Ethyl-3-methylimidazolium 2-(2-Ethoxyethoxy)ethylsulfate and 1-Butyl-3-methylimidazolium 2-(2-Methoxyethoxy)ethylsulfate, with Compressed CO_2

Andreas Hebach, Alexander Oberhof, Nicolaus Dahmen,* and Pia Griesheimer

Institute for Technical Chemistry-CPV − Forschungszentrum Karlsruhe GmbH, P.O. Box 3640, 76021 Karlsruhe, Germany

In this work, the interfacial tension (IFT) of a two-phase system consisting of compressed carbon dioxide (CO_2) and two imidazolium-based ionic liquids (ILs), 1-ethyl-3-methylimidazolium 2-(2-ethoxyethoxy)-ethylsulfate (**1**) and 1-butyl-3-methylimidazolium 2-(2-methoxyethoxy)ethylsulfate (**2**), was measured in the pressure range of (0.1 to 20) MPa at (280, 300, and 320) K. The quasi-static procedure of the pendant drop method was used. The IFT follows the general trend, that is, receding values at increasing pressure and decreasing temperature. The formation of bubbles in the IL phase and visible phase instabilities during mutual saturation of the phases suggest a high enthalpy of mixing. The viscosity of substance **2** significantly changed under CO_2 pressure. No chemical reaction is visible in the IR spectrum. Therefore, this increase in viscosity results from the formation of a new solid phase.

Introduction

Ionic liquids (ILs) have received increased attention in recent years as green solvents to be used under ambient conditions.[1] These compounds are organic salts, which are liquid at or near room temperature. ILs have no effective vapor pressure, and hence there has been considerable interest in using them in place of volatile organic compounds.[2] Therefore, ILs are considered to be an alternative media for chemical reactions exhibiting potential advantages, for example, by easy recovery and recycling of solvents.[3] Another option is the use of ILs in multiphase catalysis to allow for a homogeneous reaction in the IL phase with another phase recovering the products. The second phase may be formed by compressed CO_2 to avoid the addition of another organic solvent. Most ILs show no traceable solubility in supercritical CO_2 ($scCO_2$); conversely, CO_2 is highly soluble in IL. For example, no traces of [bmim][PF_6] could be extracted at 13.8 MPa and 313 K, but a single phase consists of 0.75 mol fraction of CO_2 at 8.3 MPa at 298 K.[4] Extraction of organic compounds using $scCO_2$ is widely used in the pharmaceutical and food industry. $ScCO_2$ is therefore discussed as an extracting medium for reaction products in ILs. Using this method would avoid cross-contamination of reaction medium and product. Accordingly, the phase behavior in the system (IL + CO_2) has been investigated.[5,6] Law et al.[7] measured the surface tension of several ILs. However, for transport processes across an interface, properties such as the interfacial tension (IFT) between the two phases are important. In this work, experimentally obtained IFT data are presented for the binary system of (CO_2 + 1-ethyl-3-methylimidazolium 2-(2-ethoxyethoxy)ethylsulfate (**1**)) and (CO_2 + 1-butyl-3-methylimidazolium 2-(2-methoxyethoxy)ethylsulfate (**2**)).

Experimental Section

Method and Apparatus. The IFT has been measured by the pendant drop method by applying the method and algorithms of Springer.[16] The apparatus used is described in detail in a previous publication on IFT measurements of the (CO_2 + water) system.[8] Briefly, the system consists of a high-pressure viewing cell with a capillary mounted to the top, which is directly fed with the IL by a precision syringe pump. A fluid circulation system driven by a gear pump provides equilibration of the CO_2 phase. The drop shapes are picked by an imaging system through borosilicate windows of the view cell. The IL is fed directly to the capillary while the view cell and high-pressure circuit are filled with CO_2. The whole system is installed in a climatic chamber, which allows a temperature adjustment within ± 0.1 K. The pressure stability is ± 0.02 MPa. Temperature is recorded within the CO_2 phase near the pending drop. The quasi-static method applied ensures a time regime where the influence of diffusion and drop aging does not affect the IFT.

A drop of IL was formed at the tip of the measuring capillary of 1.6 mm o.d. and 0.25 mm i.d.. Mutual mixing was rapid because the ILs are nearly insoluble in CO_2. In addition, the saturation of the IL with CO_2 is exothermic and results in visible convection of the drop. If there was no change within the limits of the experimental error, then the IFT data were recorded. Thereafter, the pressure was raised by the addition of CO_2 for the next pressure step up to a maximum of 20 MPa. In this way, IFT native raw data, σ_n, related to a density difference of 1000 $kg \cdot m^{-3}$ between the phases are obtained.

To calculate the actual IFT values, the density differences between the CO_2 phase and the IL phase had to be determined. Because of the negligible solubility of IL in CO_2, pure substance data have been used for the CO_2 phase, which are included in Table 1.[15] It should be mentioned that depending on the temperature and pressure adjusted, either gaseous, liquid, or $scCO_2$ was in contact with the IL. The density of the IL phase in contact with CO_2 had to be measured because a significant deviation from the pure substance data could be expected as a result of the high gas solubility under pressure. We performed density measurements by using a mass flow meter device consisting of a high-pressure view cell, circulation gear pump, and a vibrating tube densitometer, which was described in more

* Corresponding author. Fax: +49 7247 822244. E-mail: nicolaus.dahmen@kit.edu.

10.1021/je8006937 CCC: $40.75
Published on Web 03/06/2009

Table 1. Measured Data of Native and Actual Interfacial Tension, σ_n and σ, at Pressures, p, of (0.1 to 20) MPa and Temperatures, T, of (280, 300, and 320) K

1-Ethyl-3-methylimidazolium 2-(2-Ethoxyethoxy)ethylsulfate (Substance **1**)									1-Ethyl-3-methylimidazolium 2-(2-Ethoxyethoxy)ethylsulfate (Substance **1**)									
p		T		ρCO_2		σ_n		σ	p		T		ρCO_2		σ_n		σ
MPa		K		kg·m^{-3}		mN·m^{-1}		mN·m^{-1}	MPa		K		kg·m^{-3}		mN·m^{-1}		mN·m^{-1}
T/K = 280									T/K = 280									
0.10	± 0.00	280.25	± 0.00	1.90	± 0.00	31.8	± 0.0	36.7	7.03	± 0.00	280.46	± 0.00	911.56	± 0.01	24.4	± 0.1	6.0
0.10	± 0.00	280.25	± 0.00	1.90	± 0.00	32.3	± 0.1	37.3	8.96	± 0.01	280.49	± 0.00	927.77	± 0.03	25.1	± 0.0	5.8
1.17	± 0.00	280.26	± 0.01	23.90	± 0.00	26.7	± 0.0	30.3	10.86	± 0.01	280.51	± 0.00	941.49	± 0.03	25.0	± 0.1	5.4
2.34	± 0.00	280.26	± 0.01	52.78	± 0.00	20.5	± 0.0	22.6	12.97	± 0.01	280.53	± 0.00	954.85	± 0.03	26.7	± 0.3	5.4
3.34	± 0.00	280.26	± 0.00	84.48	± 0.00	14.4	± 0.0	15.5	15.11	± 0.02	280.54	± 0.00	967.03	± 0.08	26.8	± 0.1	5.1
3.95	± 0.01	280.28	± 0.01	109.93	± 0.25	9.3	± 0.0	9.8	17.29	± 0.02	280.55	± 0.00	978.21	± 0.11	28.5	± 0.1	5.1
4.24	± 0.00	280.40	± 0.02	881.34	± 0.14	22.9	± 0.1	6.3	20.67	± 0.03	280.58	± 0.00	993.76	± 0.13	28.5	± 0.1	4.7
5.23	± 0.01	280.46	± 0.01	893.11	± 0.03	24.7	± 0.1	6.6									
T/K = 299									T/K = 299									
0.10	± 0.00	299.40	± 0.00	1.78	± 0.00	31.3	± 0.1	36.2	12.35	± 0.01	299.54	± 0.01	840.14	± 0.06	21.5	± 0.1	6.8
4.81	± 0.00	299.43	± 0.01	121.43	± 0.16	14.4	± 0.0	14.9	14.74	± 0.01	299.43	± 0.00	866.67	± 0.05	22.6	± 0.0	6.6
6.68	± 0.01	299.47	± 0.01	693.95	± 0.39	18.5	± 0.1	8.6	16.39	± 0.01	299.45	± 0.00	881.25	± 0.06	23.2	± 0.0	6.4
8.33	± 0.01	299.55	± 0.01	769.00	± 0.08	20.2	± 0.1	7.9	17.88	± 0.01	299.46	± 0.00	893.13	± 0.06	23.5	± 0.0	6.2
10.23	± 0.01	299.53	± 0.01	809.85	± 0.06	21.9	± 0.1	7.6	20.36	± 0.02	299.48	± 0.01	910.42	± 0.08	24.3	± 0.0	6.0
T/K = 319									T/K = 319									
0.10	± 0.00	319.75	± 0.00	1.66	± 0.00	30.7	± 0.0	35.5	7.26	± 0.01	319.78	± 0.00	191.59	± 0.45	13.6	± 0.1	13.1
0.10	± 0.00	319.75	± 0.00	1.66	± 0.00	30.6	± 0.1	35.4	8.95	± 0.01	319.76	± 0.01	310.77	± 0.55	9.0	± 0.0	7.6
1.01	± 0.00	319.75	± 0.00	17.43	± 0.00	27.6	± 0.0	31.5	10.74	± 0.02	319.87	± 0.02	545.72	± 1.37	15.9	± 0.0	9.8
2.00	± 0.01	319.74	± 0.00	36.03	± 0.11	25.4	± 0.0	28.5	12.43	± 0.03	319.87	± 0.01	653.60	± 1.28	17.7	± 0.0	8.9
3.09	± 0.01	319.74	± 0.00	58.85	± 0.21	22.8	± 0.0	25.1	14.47	± 0.01	319.95	± 0.00	715.42	± 0.21	19.0	± 0.0	8.4
4.04	± 0.01	319.74	± 0.00	81.54	± 0.27	20.6	± 0.0	22.2	17.41	± 0.00	319.98	± 0.00	769.30	± 0.02	20.1	± 0.0	7.8
5.01	± 0.01	319.75	± 0.01	107.67	± 0.37	18.5	± 0.0	19.4	20.79	± 0.01	320.03	± 0.00	810.76	± 0.04	22.1	± 0.0	7.7
5.95	± 0.01	319.76	± 0.00	137.63	± 0.42	16.2	± 0.1	16.5									

1-Butyl-3-methylimidazolium 2-(2-Methoxyethoxy)ethylsulfate (Substance **2**)									1-Butyl-3-methylimidazolium 2-(2-Methoxyethoxy)ethylsulfate (Substance **2**)									
p		T		ρCO_2		σ_n		σ	p		T		ρCO_2		σ_n		σ
MPa		K		kg·m^{-3}		mN·m^{-1}		mN·m^{-1}	MPa		K		kg·m^{-3}		mN·m^{-1}		mN·m^{-1}
T/K = 281									T/K = 281									
0.10	± 0.00	281.31	± 0.00	1.89	± 0.00	29.3	± 0.0	34.5	5.10	± 0.01	281.58	± 0.01	882.85	± 0.04	15.0	± 0.1	4.5
1.11	± 0.00	281.32	± 0.00	22.47	± 0.00	24.3	± 0.1	28.2	6.97	± 0.02	281.58	± 0.01	903.55	± 0.12	16.1	± 0.1	4.5
1.96	± 0.01	281.30	± 0.00	42.48	± 0.18	20.2	± 0.1	23.0	9.89	± 0.03	281.61	± 0.01	928.44	± 0.14	15.7	± 0.1	4.0
3.15	± 0.01	281.31	± 0.00	77.15	± 0.17	13.7	± 0.0	15.1	13.70	± 0.04	281.61	± 0.00	953.93	± 0.20	16.8	± 0.0	3.8
3.68	± 0.00	281.30	± 0.02	96.78	± 0.02	9.9	± 0.1	10.8	17.00	± 0.05	281.63	± 0.01	972.05	± 0.21	17.8	± 0.1	3.7
4.30	± 0.00	281.48	± 0.02	873.27	± 0.00	14.8	± 0.1	4.6	19.93	± 0.06	281.63	± 0.00	986.16	± 0.24	18.1	± 0.0	3.5
T/K = 281									T/K = 281									
0.10	± 0.00	281.69	± 0.00	1.89	± 0.00	29.1	± 0.0	34.3	4.34	± 0.00	281.84	± 0.01	870.67	± 0.00	15.7	± 0.0	4.9
0.60	± 0.00	281.70	± 0.00	11.71	± 0.00	26.1	± 0.0	30.6	5.90	± 0.05	281.87	± 0.01	890.19	± 0.46	16.2	± 0.0	4.7
1.49	± 0.00	281.69	± 0.00	30.97	± 0.00	22.0	± 0.0	25.4	12.13	± 0.04	281.86	± 0.00	942.89	± 0.25	18.5	± 0.1	4.4
2.83	± 0.00	281.70	± 0.00	66.47	± 0.00	15.5	± 0.0	17.3	18.06	± 0.07	281.91	± 0.02	976.16	± 0.28	18.2	± 0.1	3.7
4.16	± 0.01	281.70	± 0.01	118.50	± 0.43	6.1	± 0.1	6.5									
T/K = 295									T/K = 295									
0.10	± 0.00	295.14	± 0.01	1.80	± 0.00	28.8	± 0.1	34.0	6.15	± 0.01	296.29	± 0.01	219.37	± 0.62	13.3	± 0.0	12.8
0.10	± 0.00	295.20	± 0.01	1.80	± 0.00	29.0	± 0.0	34.2	6.63	± 0.02	296.31	± 0.01	757.83	± 0.49	13.8	± 0.0	5.8
1.03	± 0.00	295.30	± 0.01	19.53	± 0.00	25.2	± 0.0	29.3	8.19	± 0.03	296.35	± 0.01	800.88	± 0.62	14.6	± 0.0	5.6
1.98	± 0.01	295.39	± 0.01	39.78	± 0.11	21.9	± 0.0	25.0	10.12	± 0.01	296.42	± 0.00	833.47	± 0.08	14.9	± 0.2	5.2
3.35	± 0.01	295.50	± 0.01	74.92	± 0.20	17.0	± 0.1	18.8	14.37	± 0.01	296.50	± 0.00	880.26	± 0.09	15.9	± 0.2	4.8
3.95	± 0.06	295.80	± 0.08	93.69	± 1.96	15.0	± 0.4	16.3	17.64	± 0.01	296.53	± 0.00	906.04	± 0.08	16.3	± 0.0	4.5
4.96	± 0.01	296.03	± 0.01	132.94	± 0.23	11.8	± 0.0	12.4									
T/K = 319									T/K = 319									
0.10	± 0.00	319.53	± 0.00	1.66	± 0.00	28.2	± 0.0	33.3	9.07	± 0.01	319.71	± 0.01	324.13	± 0.51	9.0	± 0.0	7.7
1.03	± 0.00	319.58	± 0.01	17.80	± 0.00	26.1	± 0.1	30.4	10.07	± 0.00	319.78	± 0.02	464.25	± 0.41	11.0	± 0.1	7.9
2.13	± 0.00	319.57	± 0.00	38.72	± 0.00	24.2	± 0.0	27.7	11.08	± 0.00	319.78	± 0.01	578.27	± 0.17	13.3	± 0.1	8.0
3.61	± 0.00	319.58	± 0.00	70.98	± 0.00	21.2	± 0.0	23.6	11.72	± 0.00	319.79	± 0.01	620.56	± 0.11	14.1	± 0.3	7.9
5.01	± 0.00	319.59	± 0.00	107.83	± 0.00	18.1	± 0.0	19.5	14.84	± 0.01	319.85	± 0.00	724.57	± 0.12	16.6	± 0.1	7.6
6.19	± 0.00	319.60	± 0.00	146.51	± 0.00	15.8	± 0.0	16.4	17.84	± 0.01	319.91	± 0.01	775.96	± 0.04	17.5	± 0.1	7.1
7.09	± 0.00	319.63	± 0.01	183.76	± 0.02	14.1	± 0.0	14.0	20.87	± 0.01	319.94	± 0.01	812.05	± 0.08	18.2	± 0.1	6.7
8.10	± 0.00	319.69	± 0.00	239.93	± 0.02	13.0	± 0.0	12.3									

detail earlier.[14] IL and CO_2 were accurately added to the system by a precision syringe. Equilibrium was attained by circulating the IL-rich phase. Afterward, the density was recorded in a temperature range between (280 and 323) K up to pressures of 20 MPa.

IR spectra were taken to check for a potential reaction between the imidazolium salt and CO_2, forming the corresponding carbonic acid. The spectra were measured using the ReactIR 1000 apparatus (ASI Applied Systems, Millersville, MD) equipped with a high-pressure cell. Prior to a measurement, the

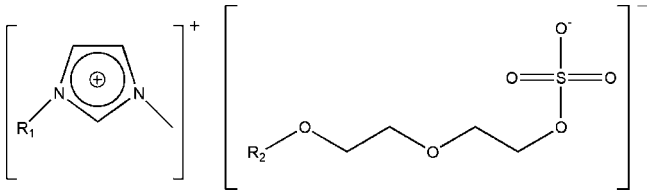

Figure 1. Schematic of the structure of **1** (R_1 = ethyl, R_2 = ethyl), **2** (R_1 = butyl, R_2 = methyl), and **3** (R_1 = ethyl, R_2 = methyl).

Table 2. Densities, ρ, for the IL Phase Estimated from Equation *2* as Used to Calculate the Density Difference, $\Delta\rho$

1-butyl-3-methylimidazolium 2-(2-ethoxyethoxy)ethylsulfate (substance **1**)		1-butyl-3-methylimidazolium 2-(2-methoxyethoxy)ethylsulfate (substance **2**)	
T	ρ	T	ρ
K	kg·m^{-3}	K	kg·m^{-3}
293	1158[a]	293	1204[b]
280	1169	282	1215
299	1154	295	1203
319	1138	319	1184

[a] Given by manufacturer. [b] Measured at STP.

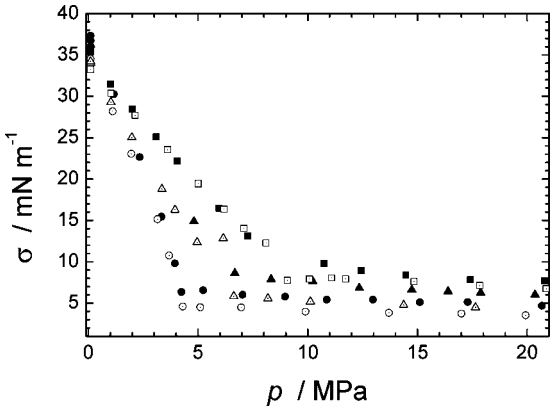

Figure 2. Measurements of the IFT, σ, of substance **1** at ●, 280 K; ▲, 299 K; ■, 319 K and of substance **2** at ⊙, 282 K; ◬, 295 K; ⊡, 319 K in the pressure range from (0.1 to 20) MPa.

system was flushed with argon. In the case of high-pressure measurements, the argon was replaced by CO_2. In addition, NMR spectra of the IL were taken before and after the experiments to watch for changes in the chemical structure.

Substances. CO_2 of 99.9999 % purity was delivered by Messer Griesheim, Karlsruhe, Germany. As IL disubstituted imidazoles, 1-ethyl-3-methylimidazolium 2-(2-ethoxyethoxy)-ethylsulfate (**1**, ECOENG 21M, ρ = 1158.35 kg·m^{-3}) and 1-butyl-3-methylimidazolium 2-(2-methoxyethoxy)ethylsulfate (**2**, ECOENG 41M, M = 310.37 g·mol^{-1}, ρ = 1181.93 kg·m^{-3}) were used. (See Figure 1.) These chemicals were supplied by Solvent Innovation GmbH (Cologne, Germany) and have been used without further cleaning. The purity of the ILs was given to be > 98 % with a water content of < 1 %.

Measuring Uncertainty. The calculation of the IFT by the computer program yields IFT raw data, σ_n, at a constant standard density difference of $\Delta\rho$ = 1000 kg·m^{-3}. The actual IFT, σ, is then obtained by equation

$$\sigma = \sigma_n \cdot \Delta\rho \tag{1}$$

In eq 1, $\Delta\rho$ is the actual density difference between the two coexisting phases under experimental conditions. It turned out to be useful to first present σ_n data, because in many cases, density data of appropriate precision are not available. To determine the uncertainty of the equipment, measurements with water and CO_2 were compared with recommended values of the ASME at atmospheric pressure. According to this comparison, the experimental uncertainty of the PeDro apparatus is less than 2 % for the determination of σ_n.

For the density determination of the IL phase, larger uncertainties of less than 5 % were estimated, mainly because of experimental factors causing difficulties in determining reliable data. At first, the gear pump caused a substantial temperature increase in the circulating fluid, which could not be compensated by the thermostatting system. Second, gas bubbles were included in the IL phase, leading to an unknown but systematic shift of the densities measured. With rising pressure, an increased gas loading of the liquid phase was observed. The density isotherms of **2** at (281 and 296) K have been terminated at pressures of 7 MPa because of a drastic increase in clouding beyond this pressure. Because of these experimental uncertainties, the liquid phase density of **1** was not measured. However, in earlier measurements with ECOENG 21M, **3**, (1-ethyl-3-methylimidazolium 2-(2-methoxyethoxy)-ethylsulfate), which differs only in having a methoxygroup instead of the ethoxygroup bonded to the anion (Figure 1), complete isotherms were obtained over the whole experimental pressure range. From the density measurements available, a simple temperature correlation was derived for interpolation of the IL phase densities at the temperatures where IFT measurements have been conducted

$$\rho_T = \rho_{STP} + m(T - T^\circ) \tag{2}$$

where ρ_{STP} and T° are the density and temperature of the pure IL at standard temperature and pressure. The parameter m has been determined from the temperature dependence of the density measurements neglecting the small pressure dependence. Because of the chemical and structural similarity between the ILs used here, the factor m is the same for both systems investigated here. The densities obtained for the IL phases by this estimate are compiled in Table 2.

Results

Interfacial Tension Measurements. The results of both σ_n and σ, as calculated by eqs 1 and 2, are presented in Table 1 and Figure 2, respectively. Both systems investigated behave alike in that there is a decrease in IFT isotherms with increasing pressure because of the large change in the density difference between the two phases. With increasing pressure, the density difference between the two phases becomes smaller and nearly constant because of the decreasing compressibility of the CO_2 phase at higher pressures. Therefore, the IFT values merge into a curve of nearly constant values. The Eötvös rule[9] is only true for low pressures, as also found for other ILs at ambient pressure, but reversed already below 1 MPa. Here IFT is increasing with increasing temperature.

The uptake of CO_2 into the IL was rapid and in connection with strong phase instabilities. Additionally, for **1**, bubbles were temporarily formed inside the drop during pressurization, sometimes forcing it to tear off from the capillary. In most cases, these bubbles vanished during the equilibration time. With **2**, a change in the drops' appearance is observed: the drop becomes opaque, and the viscosity of the IL phase apparently increased considerably and became solidlike. (See Figure 3.) The time for attaining equilibrium was more than doubled in these cases.

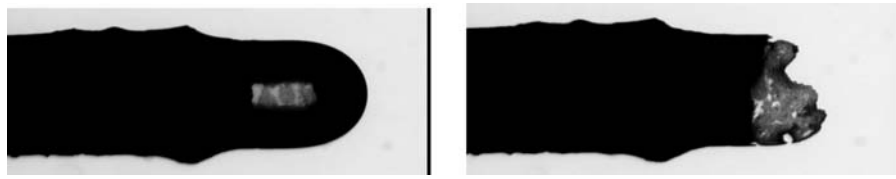

Figure 3. Image of the pendant drop of substance **2** at 282 K and 4.1 MPa.

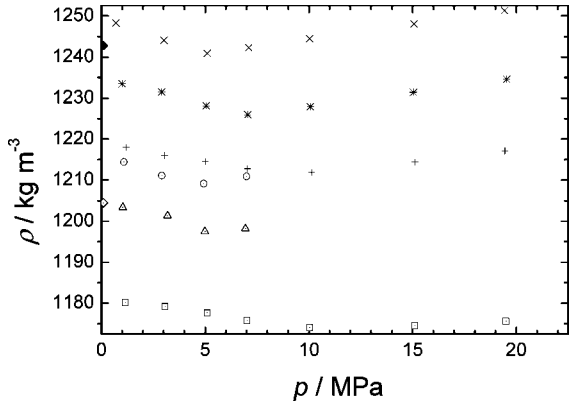

Figure 4. IL-phase density, ρ, with **2** at ⊙, 282 K; ⟁, 296 K; ⊡, 324 K and with **3** at ×, 282 K; *, 301 K; +, 322 K and within a pressure range from (1 to 20) MPa. Pure substance densities of **2** (dotted tilted square) and **3** (◆) at STP.

This increase in viscosity was also found in a NMR-sapphire tube test, where the IL was pressurized, changing the viscosity from water- to honeylike. If the pressure was released, then the initial appearance was retained.

Density Measurements. The densities of the IL phase, measured with substances **2** and **3** in contact with pressurized CO_2, are shown in Figure 4. Although the changes are small, a significant drop in the densities with increasing pressure can be observed up to around 7 MPa, after which the values slightly increase. The decrease can be explained by the observed considerable uptake of CO_2 into the IL phase at lower pressures according to the findings of phase equilibria of other authors. At higher pressures, the expected increase in density with rising pressure by compression is observed. From these data, the temperature correlation, introduced above, has been derived.

Infrared Measurements. The IR spectrum of the ILs was measured at room temperature and at 283 K first under an argon atmosphere. Thereafter, argon was replaced by CO_2 with typical 6 MPa pressure. No change in the IR spectra of **1** and **2** was observed, proving that no chemical reaction with CO_2 occurred. Also, no changes in the NMR spectra have been observed.

Discussion

Advantages of supercritical reaction media such as $scCO_2$ versus conventional solvents like hexane include high diffusion rates and gas solubility, allowing for fast and homogeneous reactions. This should lead to higher turnover frequency (TOF) for reactions that proceed under diffusion control.

Liu et al.[10] compared the hydrogenation of dec-1-ene and cyclohexene in $scCO_2$ and hexane using Wilkinson's catalyst and [bmim][PF_6]. There was nearly no reactivity advantage for $scCO_2$ because diffusion is not decisive. Hu et al.[11] compared the hydroformylation of methyl, butyl, and *t*-butyl acrylates using Rh−P(*p*-$C_6H_4C_6F_{13}$)$_3$ as a catalyst in toluene and $scCO_2$. The reaction was performed under the same temperature, pressure, and olefin concentration. This reaction proceeds under diffusion control; accordingly, we observed a much higher TOF and conversion rate in $scCO_2$.

However, high diffusion rates in the CO_2 + IL system may be hindered because of a viscosity increase in the system, a mass transfer resistance in the interface, or both. Seddon et al.[12] investigated the effect of toluene on the viscosity of [bmim][BF_4] and [bmim][PF_6]. The viscosity decreases with increasing amount of cosolvent. This seems to be a general trend because it was determined for ethanenitrile and methanol as well. But even if the solvent strength of toluene is comparable to that of $scCO_2$, there is a fundamental difference between CO_2 and organic liquids as cosolvent, for example, the possible formation of gas hydrates in the presence of water under certain conditions.

Law et al.[7] measured the surface tension of a series of related IL (bmim, omim, and C_{12}mim with anions PF_6^-, BF_4^-, Cl^-, or Br^-) using a DuNouy tensiometer. The measurements were performed at ambient pressure at various temperatures. In general, for [$C_n$mim] ILs containing the same anion, surface tension decreases with increasing alkyl chain length. We measured the IFT of **1** and **2** with CO_2 at three different temperatures in the pressure range of (0.1 to 20) MPa. (See Figure 2.) The temperature influence is identical; at constant pressure, the lower IFT is observed for **2**, which incorporates a butyl instead of an ethyl group. The pressure influence is typical for liquids + CO_2 systems.[8,13] With increasing pressure, the density of CO_2 increases. Because the IFT is proportional to the gradient of the squared density difference perpendicular to the interface and the increase in density of a liquid is much smaller than that of CO_2, the density difference diminishes and the IFT is lowered. A low IFT value favors mass transfer across the interface, so reaction and extraction would be enhanced.

However, an increase in viscosity increases the mass transfer resistance. The visually observed viscosity increase of substance **2** may be due to a reversible chemical reaction or a change in structure. Because there was no change in IR or NMR spectra, the formation of a solid phase is likely the reason. The evidence of a new, solidlike structure is shown in Figure 3. The solid formation starts at the interface IL/CO_2 and results in a tubelike structure. This structure was observed at 282 K and 4.1 MPa. It dissolves again if a rapid IL flux, causing a local temperature increase, was applied. The formation of this structure would limit the application potential of IL.

In addition, during the density measurements, it appeared that the IL phase formed quite stable emulsions with CO_2. The measurements had to be interrupted because a proper phase separation in the view cell could not be achieved.

Conclusions

The IFT of two similar ILs in compressed carbon dioxide has been measured. The principle trend in IFT with pressure and temperature is in accordance with the findings of other systems involving CO_2 and a liquid. But despite their similarity in structure, their phase behavior strongly varies. The system consisting of 1-butyl-3-methylimidazolium 2-(2-methoxyethoxy)-ethylsulfate and CO_2 undergoes a phase transition that is indefinable so far. At 282 K and 4.1 MPa, a new solid phase is formed. This phase should be similar to gas hydrates. From these findings, it is obvious that thorough investigations of the physical

properties of the IL reaction systems such as phase equilibria, viscosity, and density measurements are necessary.

Without overrating the effect found in this work, it is foreseeable that the use of CO_2 as an extracting agent to separate substances from ILs could cause severe problems in designing an appropriate process technology. On one hand, extraction kinetics may be hindered because of viscosity effects. On the other hand, phase contacting and separation may become difficult because of emulsion and foam formation. Therefore, not only the chemical and physicochemical aspects but also the process design aspects must be considered in the future work.

Literature Cited

(1) *Ionic Liquids in Synthesis*; Wasserscheid, P., Welton, T., Eds.; Wiley-VCH: Weinheim, Germany, 2002.

(2) Renner, R. An Environmental Solution. *Sci. Am.* **2001**, *285*, 13.

(3) Blanchard, L. A.; Brennecke, J. F. Recovery of Organic Products from Ionic Liquids Using Supercritical Carbon Dioxide. *Ind. Eng. Chem. Res.* **2001**, *40*, 287.

(4) Blanchard, L. A.; Hancu, D.; Beckman, E. J.; Brennecke, J. F. Green Processing Using Ionic Liquids and CO_2. *Nature* **1999**, *399*, 28.

(5) Shariati, A.; Peters, C. J. High-Pressure Phase Behavior of Systems with Ionic Liquids: II. The Binary System Carbon Dioxide + 1-Ethyl-3-methylimidazolium Hexafluorophosphate. *J. Supercrit. Fluids* **2004**, *29*, 43–48.

(6) Blanchard, L. A.; Gu, Z.; Brennecke, J. F. High Pressure Phase Behaviour of Ionic Liquid/CO_2 Systems. *J. Phys. Chem. B* **2001**, *105*, 2437–2444.

(7) Law, G.; Watson, P. R. Surface Tension Measurements of *N*-Alkylimidazolium Ionic Liquids. *Langmuir* **2001**, *17*, 6138–6141.

(8) Hebach, A.; Oberhof, A.; Dahmen, N.; Kögel, A.; Ederer, N.; Dinjus, E. Interfacial Tension at Elevated Pressures: Measurements and Correlations in the Water + Carbon Dioxide System. *J. Chem. Eng. Data* **2002**, *47*, 1540–1546.

(9) Eötvös, R. Über den Zusammenhang der Oberflächenspannung der Flüssigkeiten mit ihrem Molekularvolumen. *Ann. Phys. (Leipzig, Ger.)* **1886**, *263*, 448–459.

(10) Liu, F.; Abrams, M. B.; Baker, R. T.; Tumas, W. Phase-Separable Catalysis using Room Temperature Ionic Liquids and Supercritical Carbon Dioxide. *Chem. Commun.* **2001**, *5*, 433–434.

(11) Hu, Y.; Chen, W.; Banet Osuna, A. M.; Stuart, A. M.; Hope, E. G.; Xiao, J. Rapid Hydroformylation of Alkyl Acrylates in Supercritical CO_2. *Chem. Commun.* **2001**, *8*, 725–726.

(12) Seddon, K. R.; Stark, A.; Torres, M.-T. Influence of Chloride, Water, and Organic Solvents on the Physical Properties of Ionic Liquids. *Pure Appl. Chem.* **2000**, *72*, 2275–2287.

(13) Jaeger, P. T. *Grenzflächen und Stofftransport in Verfahrenstechnischen Prozessen am Beispiel der Hochdruck: Gegenstromfraktionierung mit überkritischem Kohlendioxid*; Shaker Verlag: Aachen, Germany, 1998.

(14) Hebach, A.; Oberhof, A.; Dahmen, N. Density of Water + Carbon Dioxide at Elevated Pressures: Measurements and Correlation. *J. Chem. Eng. Data* **2004**, *49*, 950–953.

(15) Span, R.; Wagner, W. A New Equation of State for Carbon Dioxide Covering the Fluid Region from the Triple Point Temperature to 1100 K at Pressures up to 800 MPa. *J. Phys. Chem. Ref. Data* **1996**, *25*, 1509–1596.

(16) Springer, J.; Song, B. Determination of Interfacial Tension from the Profile of a Pendant Drop Using Computer-Aided Image Processing. *J. Colloid Interface Sci.* **1996**, *184*, 64–76, 77−91.

(17) Tong, J.; Hong, M.; Guan, W.; Li, J. B.; Yang, J.-Z. Studies on the Thermodynamic Properties of New Ionic Liquids: 1-Methyl-3-pentylimidazolium Salts Containing Metal of Group III. *J. Chem. Thermodyn.* **2006**, *38*, 1416–1421.

Received for review September 17, 2008. Accepted February 9, 2009.

JE8006937